Eur. Phys. J. C manuscript No.
(will be inserted by the editor)

arXiv:1302.4606v1 [hep-ph] 19 Feb 2013

Neutral current Drell–Yan with combined QCD and electroweak corrections in the POWHEG BOX

Luca Barzè[a,1], **Guido Montagna**[b,2], **Paolo Nason**[c,3], **Oreste Nicrosini**[d,4],
Fulvio Piccinini[e,4], **Alessandro Vicini**[f,5,1]

[1]PH-TH Department, CERN, CH 1211, Geneva 23, Switzerland
[2]Dipartimento di Fisica, Università di Pavia and INFN, Sezione di Pavia, Via A. Bassi 6, 27100 Pavia, Italy
[3]INFN, Sezione di Milano Bicocca and Dipartimento di Fisica, Università di Milano Bicocca, 20133 Milano, Italy
[4]INFN, Sezione di Pavia, Via A. Bassi 6, 27100 Pavia, Italy
[5]Dipartimento di Fisica, Università di Milano and INFN, Sezione di Milano, Via Celoria 16, 20133 Milano, Italy

Received: date / Accepted: date

Abstract Following recent work on the combination of electroweak and strong radiative corrections to single W-boson hadroproduction in the POWHEG BOX framework, we generalize the above treatment to cover the neutral current Drell-Yan process. According to the POWHEG method, we combine both the next-to-leading order (NLO) electroweak and QED multiple photon corrections with the native NLO and Parton Shower QCD contributions. We show comparisons with the predictions of the electroweak generator HORACE, to validate the reliability and accuracy of the approach. We also present phenomenological results obtained with the new tool for physics studies at the LHC.

Keywords Hadron colliders · Drell-Yan · QCD · Electroweak corrections

PACS 12.15-y · 12.15.Lk · 12.38-t · 12.38.Bx · 13.85.-t

1 Introduction

The majority of the searches and studies at the proton-proton (pp) collider LHC at CERN, including the analyses related to the Higgs boson, is based on an intensive use of Parton Shower (PS) generators matched with fixed-order perturbative calculations. The success of these general computational frameworks, like MC@NLO [1] and POWHEG [2, 3], rests on their capability to provide reliable predictions for both inclusive cross sections and distributions of a large variety of signatures in the presence of arbitrary event selection conditions. The increased theoretical accuracy with respect to traditional PS generators has promoted the wide use of these frameworks on the experimental side. Generally speaking, the processes available in such tools include finite-order contributions at the next-to-leading order (NLO) accuracy in QCD [4]. Only recently the implementation of electroweak (EW) contributions in matched PS generators has been addressed in the literature [5, 6] in the process of single W-boson hadroproduction, according to the matching approach given by the POWHEG method. High precision in the W hadroproduction process is required in particular by the need to reduce theoretical uncertainties in W mass measurements. The two implementations described in Refs. [5, 6] are both available as subprocesses in the repository[1] of the general computer framework POWHEG BOX [7].

For many physics studies at the LHC, also the process of lepton pair production in hadronic collisions, known as neutral current Drell-Yan (NC DY), requires high theoretical accuracy. The state of the art of fixed-order calculations is encoded in the next-to-next-to-leading order (NNLO) QCD programs DYNNLO [8] and FEWZ [9, 10], in the EW codes HORACE [11, 12] and ZGRAD/ZGRAD2 [13, 14], while the SANC framework [15–18] and the RADY code [19] allow to evaluate both QCD and EW NLO corrections. Recently, NNLO QCD corrections were combined with NLO EW contributions in FEWZ [20].

All these theoretical efforts were made because, given the high-precision measurement of the Z-boson mass at LEP, the NC process is very helpful, if not unavoidable, for detector calibration purposes at LHC and is a standard candle that can be used to constrain the Parton Distribution Functions (PDFs). Moreover, the transverse momentum distribution of the Z boson can be accurately measured, and used to tune non-perturbative parameters in the generators.

---

[a]e-mail: luca.barze@cern.ch
[b]e-mail: guido.montagna@pv.infn.it
[c]e-mail: paolo.nason@mib.infn.it
[d]e-mail: oreste.nicrosini@pv.infn.it
[e]e-mail: fulvio.piccinini@pv.infn.it
[f]e-mail: alessandro.vicini@mi.infn.it

[1] See http://powhegbox.mib.infn.it for an updated list of all available processes.

This measurement indirectly constrains the transverse momentum distribution of the W boson, with an accuracy that strictly depends upon the accuracy of the production model. The NC DY process also allows to perform tests of the SM at the loop level and to measure EW parameters, such as the weak mixing angle, in a hadronic environment. In the high tail of the transverse momentum and invariant mass distributions of the produced leptons, the NC DY is one of the main irreducible backgrounds to the searches for new particles at the LHC.

These physics motivations require the simultaneous control of all the relevant QCD and EW higher-order contributions to the NC DY process. Following the recent implementation of EW corrections to W production in the POWHEG BOX as described in Ref. [5], here we present the analogous treatment for the NC DY process. In particular, the phenomenological importance of combining QCD and EW corrections to dilepton hadroproduction is illustrated through the analysis of various numerical results. Let us note that our approach is complementary to the combination of NLO EW corrections to NC DY with fixed-order QCD at NLO and NNLO accuracy as recently realized in the SANC framework [17, 18] and in the FEWZ code [20], respectively[2]. However, unlike the above combinations, QCD and QED shower effects are taken into account in our realization. Thanks to it, it is therefore possible to obtain reliable predictions in the presence of combined QCD and EW effects also for experimentally relevant observables, such as the Z and lepton transverse momentum, which are not realistically accessible to the tools including fixed-order corrections only.

The paper is organized as follows. In Section 2 we describe the modifications applied to the POWHEG BOX for the inclusion of the NLO EW and higher-order QED corrections in the NC DY channel. In Section 3 we present and discuss several numerical results obtained with the new tool at LHC energies, both as a cross-check of the EW corrections at NLO accuracy and about the interplay of QCD, QED and weak corrections. Conclusions are given in Section 4.

2 Details of the calculation

POWHEG (POsitive Weight Hardest Emission Generator) is a method conceived for embedding NLO QCD computations into PS simulations. Here we just review the basic ingredients and ideas of the method, paying particular attention to the components that we generalized for the inclusion of the EW and QED corrections. For more details the reader is referred to the original literature [2, 3, 7].

2.1 The POWHEG method

In the POWHEG formalism, the generation of the hardest emission is performed first, using full NLO accuracy, and a shower Monte Carlo is used to generate subsequent radiation. Therefore, the building blocks of the method are those typical of a NLO calculation and of PS generators.

At NLO accuracy in QCD, the necessary ingredients are given by the process-dependent virtual corrections V_{QCD} and real radiation matrix element(s) R_{QCD}. To ensure cancellation of the initial-state collinear singularities in hadronic collisions, further components of the calculation are two factorization counterterms, one for each of the incoming partons $(\oplus,\ominus)$, which we denote, following the POWHEG notation, as $G^{QCD}_{\oplus,\ominus}$ (the collinear remnants). Soft and collinear divergences coming from real radiation are treated in POWHEG using a subtraction method (the FKS subtraction formalism [28]) which requires the introduction of a set of functions $C^{(\alpha)}_{QCD}$ (the real counterterms), where the superscript α denotes a particular singular region of R_{QCD}. Correspondingly, the method requires that the real radiation contribution is separated in all those terms R^{α}_{QCD} that are only singular in a single region α.

With all these ingredients at hand, the calculation of an inclusive cross section with NLO QCD accuracy proceeds in the POWHEG BOX according to a high degree of automation. First the algorithm identifies all the singular regions and maps the real radiation matrix element over the singular configurations. Afterwards, it performs the subtraction procedure and computes the collinear remnants. As shown in the following, this procedure can be effectively generalized to the inclusion of EW contributions, provided the appropriate ingredients and modifications are supplied.

In the POWHEG method, the matching of the NLO computation with the PS is achieved in terms of a modified Sudakov form factor, which contains the NLO real radiation matrix element and is equal to the product of the Sudakov form factors for each singular region. The generation of the event with the hardest radiation, which is a fundamental aspect of the approach, is also handled automatically by the POWHEG BOX framework and can be adapted to cope with the radiation of colorless partons, as discussed in the following.

2.2 Electroweak contributions: calculation and inclusion in the POWHEG BOX

We treated the NC DY process according to the same recipe adopted in Ref. [5] for the implementation of the EW contributions to single W production in the POWHEG BOX.

The most intricate and lengthy step is the calculation of the one-loop EW corrections V_{EW}, since it involves the treatment of unstable particles in addition to the cancellation of mass singularities. We accomplished this task realizing a library for the computation of V_{EW}, based upon the one-loop structure for the virtual photonic and weak corrections given in Ref. [19]. Unlike Ref. [19], where mass regularization is used to treat soft and collinear singularities, we employed a mixed scheme in order to comply with the use of dimensional regularization of POWHEG. Precisely, we used dimensional regularization to treat the singularities associated to the QCD partons and the photon, but we kept the mass of the leptons finite, since this mass has a well-defined physical meaning, being the true regulator of the QED mass singularities. For the evaluation of the scalar integrals, we resorted in particular to various results of Ref. [29] (for the computation of the three-point functions) and Ref. [30] (for the computation of the four-point functions).

---

[2] Further studies on combining QCD and EW corrections to W/Z hadroproduction are described in Refs. [21–27]

The singularities associated to the unstable nature of the weak bosons circulating in the loops and given by logarithms of the form $\log(s - M_V^2 + i\varepsilon)$ were treated according to two different schemes, which both respect gauge invariance. In the first approach (factorization scheme) [19, 31], the logarithms that are singular at the resonance (and would be cured by a Dyson resummation of the self-energy contributions inside the loop diagrams) are treated with the substitution $\log(s - M_V^2 + i\varepsilon) \to \log(s - M_V^2 + i\Gamma_V M_V), V = W, Z$. In the second approach (complex mass scheme) [32, 33], the squared vector boson masses are taken as complex quantities $\mu_{W,Z}^2 = M_{W,Z}^2 - i\Gamma_{W,Z} M_{W,Z}$ in the LO and NLO calculation, leading to complex couplings as well. Both schemes were implemented in the POWHEG BOX and the differences between the two procedures for treating the resonance are at the per mille level or below it for arbitrary partonic centre of mass (c.m.) energies $\hat{s}$ [19].

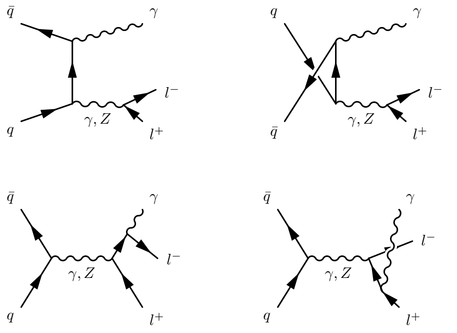

Fig. 1 The photon bremsstrahlung diagrams of the NC DY process.

To complete the NLO EW calculation, we computed the real photon matrix element R_{EW} relative to the bremsstrahlung processes $q\bar{q} \to \gamma, Z \to\to l^+ l^- \gamma$ shown in Fig. 1. We included finite lepton mass effects in the calculation and resorted to the algorithm developed and described in detail in Ref. [5] for the treatment of the radiation phase space with massive fermions. The search for the singular regions was extended to handle the divergences associated to photon radiation. The original algorithm applied to the initial-state radiation (ISR) of QCD partons was generalized to treat the mechanisms of QED ISR and final-state radiation (FSR). As the large logarithms associated to photon ISR have to be reabsorbed in the PDFs, in analogy to QCD, the dominant QED contribution is due to FSR, which contains logarithms of the form $\alpha_{\rm em} \log(\hat{s}/m_l^2)$ for the typical non-fully inclusive and non-infrared safe conditions used in the event selection. As demonstrated in Ref. [5], the new phase space treatment including massive leptons is a key ingredient to take under control the above logarithmic contributions. To ensure cancellation of all the mass singularities in terms of the new phase space, we also recalculated the QCD matrix element R_{QCD} including finite lepton mass contributions in the calculation of both the gluon emission $q\bar{q} \to \gamma, Z \to\to l^+ l^- g$ and gluon-induced $gq/\bar{q} \to l^+ l^- q/\bar{q}$ processes.

To summarize, the implementation of EW corrections in the POWHEG BOX was realized through the following generalization of the native QCD elements

$$\begin{aligned}
& V_{QCD} \to V_{QCD} + V_{EW} \\
& R_{QCD} \to R_{QCD} + R_{EW} \\
& C_{QCD}^{(\alpha)} \to C_{QCD}^{(\alpha)} + C_{EW}^{(\alpha)} \\
& G_{\oplus,\ominus}^{QCD} \to G_{\oplus,\ominus}^{QCD} + G_{\oplus,\ominus}^{EW}
\end{aligned} \qquad (1)$$

and improving the algorithm for the identification of the singular regions associated to real photon radiation.

For the cross section calculation, we implemented three input parameter schemes: the G_μ, the on-shell $\alpha_{\rm em}(0)$ and the $\alpha_{\rm em}(M_Z)$ scheme. In the first scheme, the primary input parameters are given by the muon decay constant and the weak boson masses; in the second one, G_μ is replaced by the fine structure constant at zero momentum transfer. In the latter scheme, the non-perturbative hadronic contribution to the running of $\alpha_{\rm em}$ is treated in terms of effective quark masses reproducing the correct value of $\alpha_{\rm em}(Q^2)$ at high energies, i.e. $Q^2 = M_Z^2$. In the third scheme, the input parameters are $\alpha_{\rm em}$ at the scale $Q^2 = M_Z^2$, M_Z and M_W. The widths of the weak bosons are kept fixed everywhere.

As a last step, we matched the NLO QCD and EW corrections with PS contributions. We considered both QCD and QED parton cascade. According to POWHEG, the generation of the hardest-radiation event is performed in terms of the exact real radiation matrix element and of a modified Sudakov form factor including it. Once the configuration with the hardest (transverse momentum $p_\perp$) emission has been generated, the subsequent radiation processes handled by the PS take place at lower $p_\perp$, applying a veto technique. The above algorithm was generalized to include photon radiation in the POWHEG BOX. We made use of both R_{QCD} and R_{EW} and implemented a Sudakov form factor equal to the product of the form factors for ISR gluon and photon radiation, as well as FSR photon radiation. In the native QCD construction, the method requires a lower cut-off on the transverse momentum, in order to avoid to reach unphysical values of the strong coupling constant and of the PDFs. Also this requirement was generalized, following the procedure applied to W production in Ref. [5]. Precisely, the lower $p_\perp$ cut-off was set equal to a typical hadronic scale for gluon or photon radiation from quarks, while it was taken as the mass of the lepton for QED radiation off the leptons. The package PHOTOS [34][3] is used to handle multiple photon emission, with enforced $p_\perp$-ordered radiation.

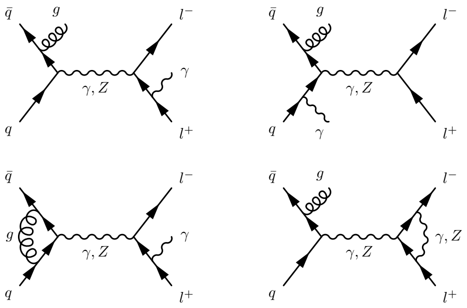

Fig. 2 Examples of mixed QCD⊗EW contributions included in the POWHEG BOX assuming factorization.

In conclusion, let us note that the inclusion of all the theoretical elements as described above allows to obtain predictions for dilepton production in hadronic collisions taking into account the interplay between QCD and EW contributions in a single computational framework. In particular, the matching of the complete NLO SM corrections with the showers of both colored particles and photons enables to perform simulations of the differential cross sections in the presence of mixed QCD⊗EW effects, in addition to the contribution of higher-order QCD and QED corrections. In the absence of a complete calculation of $O(\alpha_{\rm em}\alpha_s)$ corrections to DY processes[4], the tool enables to obtain, using factorization, leading logarithmic predictions for mixed QCD⊗EW contributions, as schematically shown in Fig. 2.

3 Phenomenological results

In this Section, we show the results of a variety of tests performed to validate the new theoretical and computational ingredients implemented in the POWHEG BOX. We first present comparisons against the benchmark predictions of the HORACE generator [11, 12] at NLO EW accuracy[5]. Then we address a phenomenological analysis of the interplay between QCD and EW corrections of interest for physics studies at the LHC.

3.1 Input parameters and event selection

We considered the lepton pair hadroproduction process $pp \to \gamma, Z \to \mu^+\mu^- + (X)$, at the c.m. energy $\sqrt{s} = 14$ TeV. We used the MRST2004QED set of PDFs [43] with renormalization and (QCD and QED) factorization scale $\mu_R = \mu_F = M_Z$ for the comparison with HORACE and the QCD⊗EW simulations around the Z resonance, and $\mu_R = \mu_F = M_{l^+l^-}$ (the lepton pair invariant mass) for the numerical results on the combination of QCD and EW corrections well above the peak. For both the final-state leptons, we applied the following cuts on the transverse momentum and pseudorapidity:

$$p_\perp^{\mu^\pm} > 20\,\text{GeV}\,, \qquad |\eta_{\mu^\pm}| < 2.5\,, \tag{2}$$

which approximately model the acceptance of the ATLAS and CMS detectors at the LHC. In addition we also applied a cut on the invariant mass of the lepton pair of $M_{l^+l^-} >$ 50 GeV. We considered, for simplicity, “bare" leptons, *i.e.* nearby photons are not recombined with the leptons. The results have been obtained in the $\alpha_{\rm em}(0)$ scheme, using the input parameters listed in Table 1[6], which coincide with those adopted in the tuned comparisons of EW predictions for Z boson observables described in Ref. [44]. The overall choice of input parameters, PDF set and acceptance cuts allowed us to check first that the NLO EW predictions of both HORACE and the new POWHEG version perfectly agree with the benchmark results for the integrated cross sections given in Ref. [44]. For the coupling of the external photons to the charged particles needed for the evaluation of the photonic corrections we used $\alpha_{\rm em} = \alpha_{\rm em}(0)$, and $\alpha_s(M_Z) = 0.1205$ with NLO evolution for the results about the combination of QCD and EW contributions.

3.2 Comparisons with HORACE

The results of the validation of the pure NLO EW corrections in the POWHEG BOX framework are shown in Figs. 3 through 6 by comparisons with HORACE simulations. The invariant mass region around the Z resonance and well above it ($M_{l^+l^-} > 1$ TeV) are considered in Fig. 3 - Fig. 4 and Fig. 5

---

[3] We use PHOTOS with leading log kernels, i.e. without process-dependent matrix element corrections already included in our approach in the exact NLO calculation.

[4] Partial results exist in the literature and are given by the one-loop EW corrections to W/Z+jet production at finite transverse momentum [35–38], NLO QCD corrections to the $W/Z+\gamma$ process [39–41] and two-loop virtual $O(\alpha_{\rm em}\alpha_s)$ corrections to the NC DY [42]. However, the complete and non-trivial combination of all the above substructures is still unavailable.

[5] Note that HORACE implements completely independent EW form factors and real photon matrix elements, computed in the mass regularization scheme.

[6] The CKM mixing matrix is set to the identity matrix in the calculation of EW loop corrections.

Table 1 The input parameters used in the numerical simulations.

$\alpha_{\text{em}}(0) = 1/137.03599911$	$M_Z = 91.1876$ GeV	$M_W = 80.37399$ GeV
$\Gamma_Z = 2.4924$ GeV	$\sin^2\theta_W = 1 - M_W^2/M_Z^2$	$M_{\text{Higgs}} = 125$ GeV
$\Gamma_W = 2.141$ GeV	$\alpha_s(M_Z) = 0.1205$	
$m_e = 510.99892$ KeV	$m_\mu = 105.658369$ MeV	$m_\tau = 1.77699$ GeV
$m_u = 0.06983$ GeV	$m_c = 1.2$ GeV	$m_t = 174$ GeV
$m_d = 0.06984$ GeV	$m_s = 150$ MeV	$m_b = 4.6$ GeV

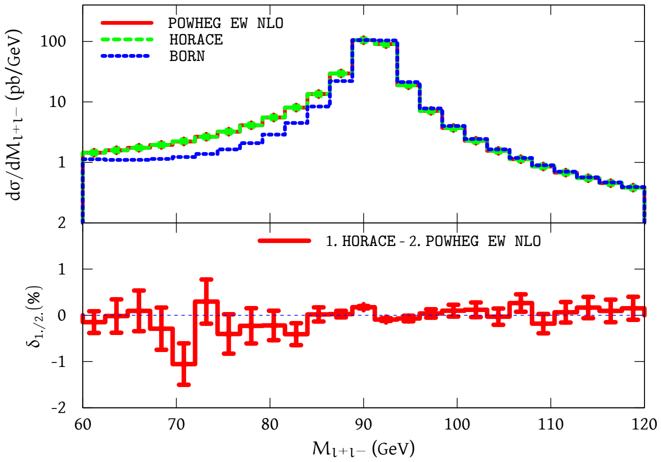

Fig. 3 Upper panel: lepton-pair invariant mass distribution according to POWHEG BOX and HORACE at NLO EW accuracy, in the resonance region. Lower panel: relative deviations, in percent, between the predictions of the two generators.

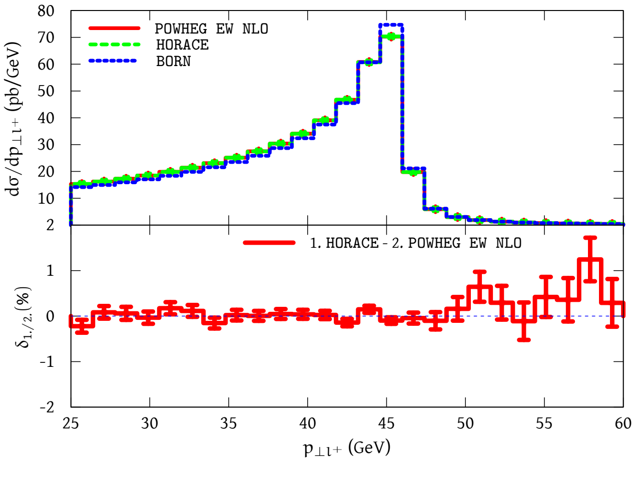

Fig. 4 The same as Fig. 3 for the lepton transverse momentum distribution.

- Fig. 6, respectively. For these comparisons we took the limit $\alpha_s \to 0$ numerically in POWHEG. In the upper panels, we show the NLO predictions of the two codes for the invariant mass and $p_\perp^l$ distributions, together with the reference Born results. The lower panels show the relative difference (in percent) between the two programs, where the error bars correspond to 1σ numerical uncertainties.

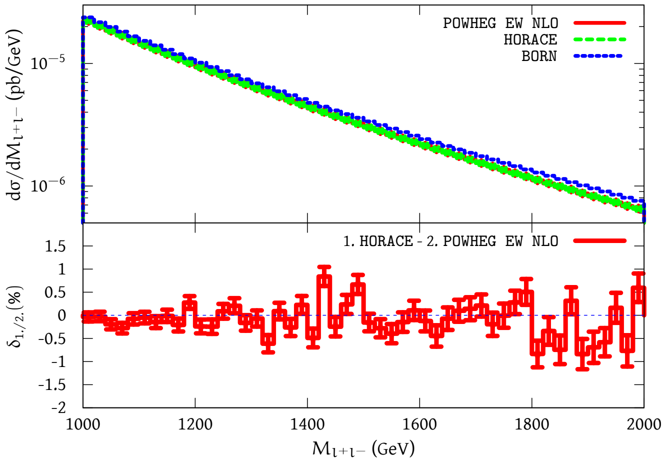

Fig. 5 The same as Fig. 3 in the region $M_{l^+l^-} > 1$ TeV.

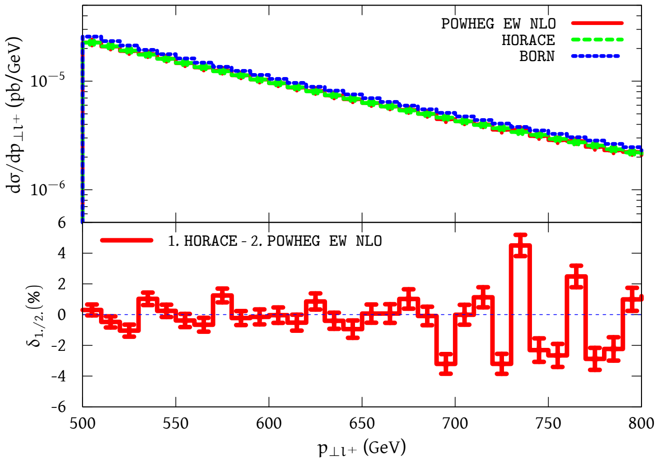

Fig. 6 The same as Fig. 5 for the lepton transverse momentum distribution.

We observe that the results of the two programs are in good agreement, both in the peak region and in the high tails. This means that all the EW ingredients have been correctly included in POWHEG. In particular, the agreement in the Z resonance region is a test of the correct calculation of the NLO virtual and real contributions, as well as of the generalized subtraction procedure and treatment of collinear photon singularities. Indeed, the EW corrections in the peak region are known to be dominated by the mechanism of final state photon radiation, which receives contributions from all the above components. On the other hand, the NLO EW corrections to the tails of the distributions give rise to large negative contributions due to Sudakov-like logarithms of the form $\alpha_{\rm em}\log(\hat{s}/M_V^2)$. The latter come from the exchange of weak gauge bosons in the loops, which therefore display in POWHEG the expected behavior at high energies[7].

In summary, the implementation in the POWHEG BOX of all the NLO EW corrections to the NC DY can be considered fully under control.

3.3 Combined effect of QCD and EW corrections

The full results of the POWHEG BOX for the combined effect of QCD and EW corrections to the invariant mass and lepton transverse momentum distribution are shown in Fig. 7 - Fig. 8 in the resonance region, and in Fig. 9 for $M_{l^+l^-} >$ 1 TeV. Further numerical results concerning the transverse momentum distribution of the Z boson in the resonance region are shown in Fig. 10 - Fig. 13, in comparison with ATLAS [49] and CMS [50] data at $\sqrt{s} = 7$ TeV.

For Fig. 7 - Fig. 9 the complete predictions have been obtained by matching the NLO QCD and EW corrections with QCD (PYTHIA version 6.4 [46]) and QED (PHOTOS) showers. For the sake of comparison, the pure QCD predictions of the standard POWHEG BOX are also given, together with the pure NLO EW results. The absolute predictions for the various distributions are shown in the upper panels of each plot. The lower panels display the relative difference, in percent, between the results of the new version of the POWHEG BOX and the standard QCD release, as well as the relative effect due to the genuine NLO EW corrections. Therefore the comparison between the two lines in each lower panel of Fig. 7 - Fig. 9 provides a measure of the QCD⊗EW factorization and, more precisely, of mixed leading logarithmic corrections at the order $\alpha_{\rm em}^m \alpha_s^n, m,n \geq 1$.

Generally speaking, one can notice that both QCD and EW corrections (and their combination) are necessary for a proper control of the normalization and shape of the distributions. Particularly, the invariant mass distribution in the resonance region receives large corrections and a significative shape modification from QED corrections, as emphasized in previous studies [12, 13, 45]. As shown in Fig. 7, the left tail of the distribution is enhanced by the mechanism of final state photon radiation by several tens of percent, while the peak value is reduced by about 20%. For this distribution the effect of the EW corrections largely exceeds that of QCD radiation, and the impact of mixed QED⊗EW contributions is substantial, especially in the left tail of the distribution. The same kind of effect is present in the forward-backward asymmetry as a function of the lepton pair invariant mass for $M_{l^+l^-}$ below the Z mass, as we checked explicitly in our simulations. For the lepton $p_\perp$ the well-known overwhelming QCD effects are by far dominant over the EW contributions, whose shape is washed out by QCD radiation (see Fig. 8). For such a distribution, the interplay of the particularly large QCD corrections with the ten percent level EW effects gives rise to mixed contributions of the order of several percents close to the peak, as clearly visible in the lower panel of Fig. 8.

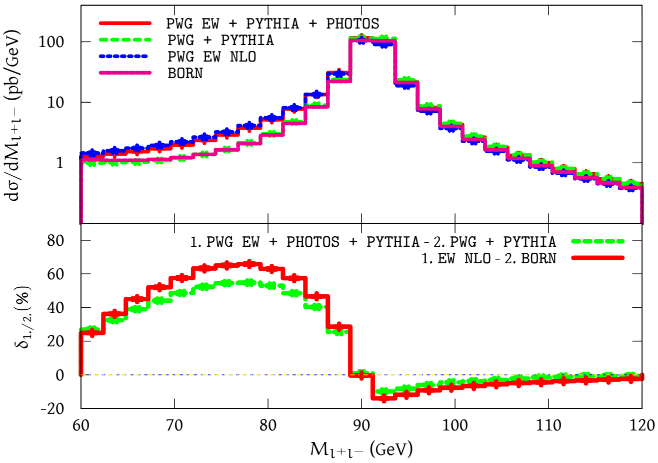

Fig. 7 Upper panel: lepton-pair invariant mass distribution around the resonance according to the full QCD⊗EW predictions of the POWHEG BOX (PWG EW + PYTHIA+PHOTOS), the standard QCD POWHEG BOX (PWG + PYTHIA), the LO and the NLO EW approximations. Lower panel: relative difference, in percent, between the full QCD⊗EW predictions and the pure QCD ones (green, dotted line), in comparison with the relative contribution due to pure NLO EW corrections (red, solid line).

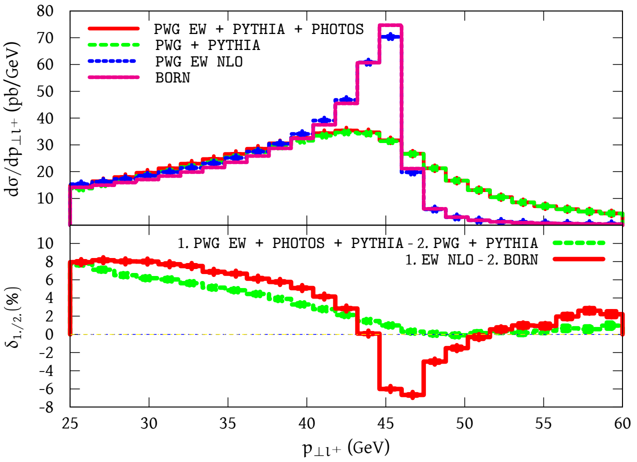

Fig. 8 The same as Fig. 7 for the lepton transverse momentum distribution.

Non-negligible QCD⊗EW corrections are also present in the very high tail of the invariant mass distribution shown in Fig. 9. In this region the large EW corrections, enhanced

---

[7] Note that we do not take into account in our calculation the contribution due to real radiation of massive gauge bosons, which is known [47, 48] to partially compensate the negative virtual Sudakov-like corrections.

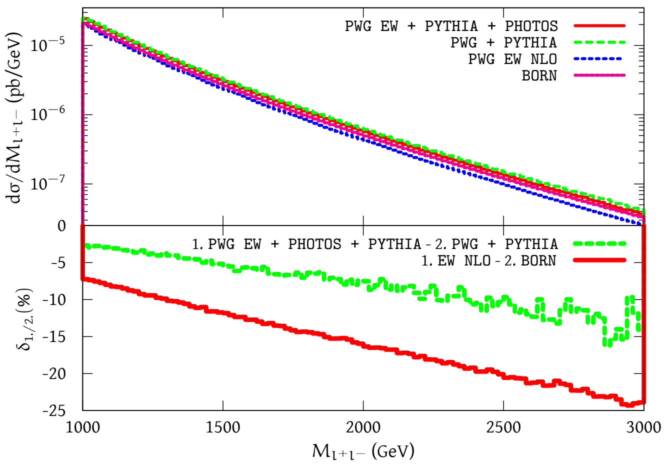

Fig. 9 The same as Fig. 7 in the region $M_{l^+l^-} > 1$ TeV.

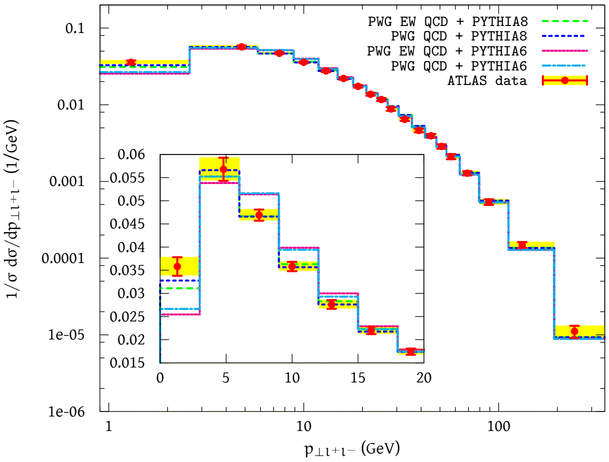

Fig. 10 The normalized differential cross section as a function of $p_\perp^Z$ for the full range up to 350 GeV (whole plot) and in the range $p_\perp^Z$ < 20 GeV (inset). The ATLAS data (for bare muons) are compared with the predictions of the POWHEG BOX with full QCD⊗EW contributions and QCD corrections only, and according to two PYTHIA versions.

by Sudakov-like logarithms, in association with QCD radiation induce mixed contributions which grow from a few to several percents, as can be seen in the lower panel of Fig. 9.

Last but not least, we show for illustrative purposes in Fig. 10 - Fig. 13 our results for the Z transverse momentum distribution, whose knowledge is crucial for a precise measurement of the W mass and whose description represents a challenge for QCD. The predictions of the POWHEG BOX are compared with ATLAS data [49] (see Fig. 10 - Fig. 11) and CMS data [50] (see Fig. 12 - Fig. 13) at $\sqrt{s}$ = 7 TeV[8]. For these results, we imposed the acceptance and invariant mass cuts quoted in the experimental papers, we focused on the data referring to bare muons and we used the MSTW2008 NLO PDF set [52]. Because of the considerable dependence of the $p_\perp^Z$ distribution on adjustable non-perturbative parameters, we considered POWHEG interfaced to two different versions of PYTHIA generator, namely PYTHIA version 6.4 [46] and version 8.1 [51]. For each PYTHIA version, we used the default values for the parameters describing the underlying event and shower effects. While higher-order QED radiation is treated with PHOTOS when POWHEG is interfaced to PYTHIA 6.4, the simulation performed with PYTHIA 8.1 uses its internal available tool for QED shower.

In Fig. 10 and Fig. 12 we show the absolute predictions of POWHEG for the normalized differential cross section as a function of $p_\perp^Z$ in comparison with ATLAS and CMS data, respectively. The POWHEG results are presented both with and without NLO EW and QED Shower corrections,

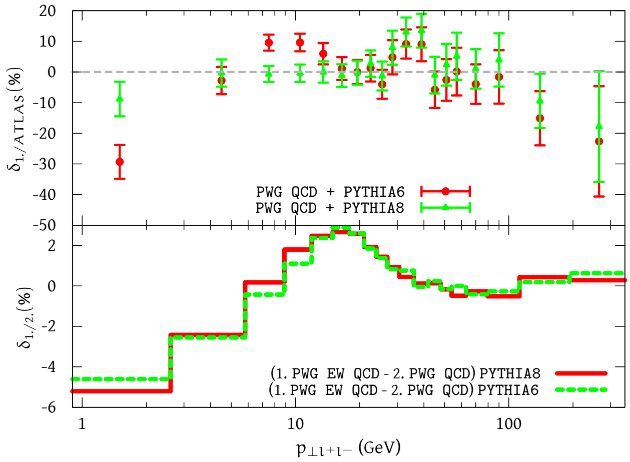

Fig. 11 Upper panel: ratio of the POWHEG BOX QCD predictions over the ATLAS data, according to two different version of PYTHIA. Lower panel: relative difference, in percent, between the full QCD⊗EW predictions and the pure QCD ones of POWHEG BOX for two different PYTHIA versions.

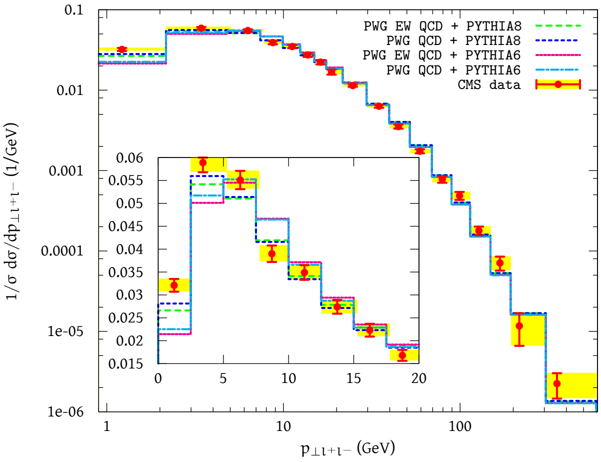

Fig. 12 The same as Fig. 10 for CMS data (for bare muons) up to 600 GeV.

---

[8] We used the data available at the HepData repository http://hepdata.cedar.ac.uk.

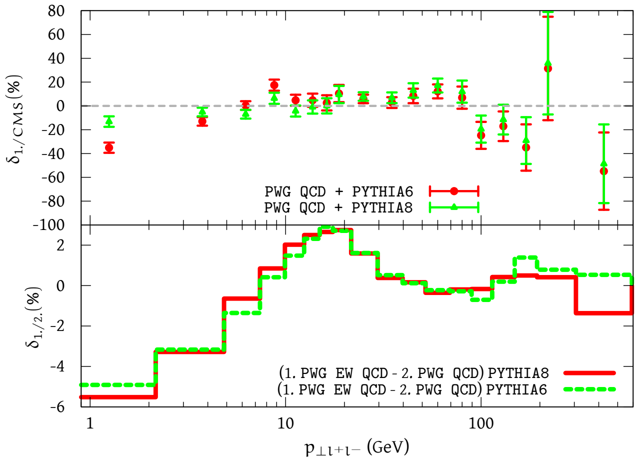

Fig. 13 The same as Fig. 11 for CMS data.

and according to the two aforementioned PYTHIA versions. The inset figures show the data-theory comparison in the low $p_\perp^Z$ region. Albeit an optimal description of the Z transverse momentum distribution over the full range seems to be problematic, there is a rather good agreement with the data, especially when considering the POWHEG BOX interfaced to PYTHIA version 8.1. The latter statement can be understood by looking at the upper panels of Fig. 11 and Fig. 13. They show the ratio of the POWHEG BOX QCD predictions over the ATLAS and CMS data, as obtained with PYTHIA version 6.4 and version 8.1, respectively. Especially in the low $p_\perp^Z$ region, POWHEG interfaced to PYTHIA 8.1 provides a much better description of the data, both for ATLAS and CMS. The lower panels of Fig. 11 and Fig. 13 show in conclusion the impact on the Z transverse momentum distribution due to NLO EW and multiple photon corrections, as well as to $O(\alpha_{\mathrm{em}}\alpha_s)$ contributions. As can be noticed, these contributions are largely independent of the particular version of the QCD/QED Shower generator under consideration. They introduce a negative correction of some percents in the first bins of the $p_\perp^Z$ distribution, while yielding a moderate effect of about +2% for $p_\perp^Z$ around 20 - 30 GeV.

As a concluding remark, it is worth noting the the possibility of simulating the contribution of mixed QCD⊗EW corrections with the new tool is due to the particular factorized form of the EW corrections in the QCD POWHEG framework. In this respect, our predictions contain complementary information with respect to the calculation of Refs. [17–20], where QCD and EW corrections are combined additively. Moreover, the approach includes details of the interplay between QCD and EW radiation which are not taken into account in the experimental procedure typically followed at the LHC of applying EW K-factors to the predictions of a reference QCD program.

4 Conclusions

We have generalized previous work on the inclusion of the EW corrections to single W production in the POWHEG BOX to cope with the NC DY process. We have added NLO EW and QED multiple photon corrections to the native NLO and PS QCD contributions. To this aim, we have exploited the process-independent structure of the POWHEG BOX framework and resorted to various general techniques already successfully developed for W-boson production.

We have provided evidence of the accuracy of the approach and presented a sample of phenomenological results about the combination of QCD and EW corrections to lepton pair production in hadronic collisions at LHC energies. In particular, we have shown that the leading contribution of mixed QCD⊗EW corrections may affect some observables at the level of several percents, beyond the separate effect of strong, weak and electromagnetic corrections. Therefore, the exact calculation of $O(\alpha_{\mathrm{em}}\alpha_s)$ corrections would be desirable for a better theoretical control of the DY cross sections.

The new tool enables to obtain precise and realistic predictions for the NC DY process, in the same way as the charged-current channel. It is available at the web site of POWHEG BOX. Further theoretical ingredients, such as photon-induced processes [12, 19, 53, 54] and presently neglected higher-order corrections, will be made available in future releases.

We expect that the results here presented will facilitate the work of experimental analysis and data interpretation at hadron colliders and will allow in the future a rather simple inclusion in the POWHEG BOX of EW effects to further processes of physics interest.

Acknowledgements We are grateful to various colleagues of the LHC and Tevatron communities for interest in our work and many useful discussions. This work was supported in part by the Research Executive Agency (REA) of the European Union under the Grant Agreement number PITN-GA-2010-264564 (LHCPhenoNet), and by the Italian Ministry of University and Research under the PRIN program 2010-2011. The work of L.B. is supported by the ERC grant 291377, “LHC-theory - Theoretical predictions and analyses of LHC physics: advancing the precision frontier". F.P. would like to thank the CERN PH-TH Department for partial support and hospitality during several stages of the work.

References

1. S. Frixione and B. R. Webber, JHEP **0206** (2002) 029, hep-ph/0204244.
2. P. Nason, JHEP **0411** (2004) 040, hep-ph/0409146.
3. S. Frixione, P. Nason and C. Oleari, JHEP **0711** (2007) 070, arXiv:0709.2092 [hep-ph].
4. P. Nason and B. Webber, Ann. Rev. Nucl. Part. Sci. **62** (2012) 187, arXiv:1202.1251 [hep-ph].

5. L. Barzè, G. Montagna, P. Nason, O. Nicrosini and F. Piccinini, JHEP **1204** (2012) 037, arXiv:1202.0465 [hep-ph].
6. C. Bernaciak and D. Wackeroth, Phys. Rev. D **85** (2012) 093003, arXiv:1201.4804 [hep-ph].
7. S. Alioli, P. Nason, C. Oleari and E. Re, JHEP **1006** (2010) 043, arXiv:1002.2581 [hep-ph].
8. S. Catani, L. Cieri, G. Ferrera, D. de Florian and M. Grazzini, Phys. Rev. Lett. **103** (2009) 082001, arXiv:0903.2120 [hep-ph].
9. K. Melnikov and F. Petriello, Phys. Rev. D **74** (2006) 114017, hep-ph/0609070.
10. R. Gavin, Y. Li, F. Petriello and S. Quackenbush, Comput. Phys. Commun. **182** (2011) 2388, arXiv:1011.3540 [hep-ph].
11. C. M. Carloni Calame, G. Montagna, O. Nicrosini and A. Vicini, JHEP **0612** (2006) 016, hep-ph/0609170.
12. C. M. Carloni Calame, G. Montagna, O. Nicrosini and A. Vicini, JHEP **0710** (2007) 109, arXiv:0710.1722 [hep-ph].
13. U. Baur, S. Keller and W. K. Sakumoto, Phys. Rev. D **57** (1998) 199 [hep-ph/9707301].
14. U. Baur, O. Brein, W. Hollik, C. Schappacher and D. Wackeroth, Phys. Rev. D **65** (2002) 033007, hep-ph/0108274.
15. A. Arbuzov, D. Bardin, S. Bondarenko, P. Christova, L. Kalinovskaya, G. Nanava and R. Sadykov, Eur. Phys. J. C **54** (2008) 451, arXiv:0711.0625 [hep-ph].
16. A. Andonov, A. Arbuzov, D. Bardin, S. Bondarenko, P. Christova, L. Kalinovskaya, V. Kolesnikov and R. Sadykov, Comput. Phys. Commun. **181** (2010) 305, arXiv:0812.4207 [physics.comp-ph].
17. D. Bardin, S. Bondarenko, P. Christova, L. Kalinovskaya, L. Rumyantsev, A. Sapronov and W. von Schlippe, JETP Lett. **96** (2012) 285, arXiv:1207.4400 [hep-ph].
18. S. G. Bondarenko and A. A. Sapronov, “NLO EW and QCD proton-proton cross section calculations with mcsanc-v1.01", arXiv:1301.3687 [hep-ph].
19. S. Dittmaier and M. Huber, JHEP **1001** (2010) 060, arXiv:0911.2329 [hep-ph].
20. Y. Li and F. Petriello, Phys. Rev. D **86** (2012) 094034, arXiv:1208.5967 [hep-ph].
21. Q. -H. Cao and C. P. Yuan, Phys. Rev. Lett. **93** (2004) 042001, hep-ph/0401026.
22. N. E. Adam, V. Halyo and S. A. Yost, JHEP **0805** (2008) 062, arXiv:0802.3251 [hep-ph].
23. N. E. Adam, V. Halyo, S. A. Yost and W. Zhu, JHEP **0809** (2008) 133, arXiv:0808.0758 [hep-ph].
24. G. Balossini, G. Montagna, C. M. Carloni Calame, M. Moretti, M. Treccani, O. Nicrosini, F. Piccinini and A. Vicini, Acta Phys. Polon. B **39** (2008) 1675, arXiv:0805.1129 [hep-ph].
25. G. Balossini, G. Montagna, C. M. Carloni Calame, M. Moretti, O. Nicrosini, F. Piccinini, M. Treccani and A. Vicini, JHEP **1001** (2010) 013, arXiv:0907.0276 [hep-ph].
26. P. Richardson, R. R. Sadykov, A. A. Sapronov, M. H. Seymour and P. Z. Skands, JHEP **1206** (2012) 090, arXiv:1011.5444 [hep-ph].
27. S. Yost, V. Halyo, M. Hejna and B. F. L. Ward, “HERWIRI2: CEEX Electroweak Corrections in a Hadronic MC”, arXiv:1201.5906 [hep-ph].
28. S. Frixione, Z. Kunszt and A. Signer, Nucl. Phys. B **467** (1996) 399, hep-ph/9512328.
29. S. Dittmaier, Nucl. Phys. B **675** (2003) 447, hep-ph/0308246.
30. A. Denner and S. Dittmaier, Nucl. Phys. B **844** (2011) 199, arXiv:1005.2076 [hep-ph].
31. S. Dittmaier and M. Kramer, Phys. Rev. D **65** (2002) 073007, hep-ph/0109062.
32. A. Denner, S. Dittmaier, M. Roth and L. H. Wieders, Nucl. Phys. B **724** (2005) 247, Erratum-ibid. B **854** (2012) 504, hep-ph/0505042.
33. A. Denner and S. Dittmaier, Nucl. Phys. Proc. Suppl. **160** (2006) 22, hep-ph/0605312.
34. P. Golonka and Z. Was, Eur. Phys. J. C **45** (2006) 97, hep-ph/0506026.
35. J. H. Kuhn, A. Kulesza, S. Pozzorini and M. Schulze, Phys. Lett. B **651** (2007) 160, hep-ph/0703283 [hep-ph].
36. J. H. Kuhn, A. Kulesza, S. Pozzorini and M. Schulze, Nucl. Phys. B **797** (2008) 27, arXiv:0708.0476 [hep-ph].
37. W. Hollik, T. Kasprzik and B. A. Kniehl, Nucl. Phys. B **790** (2008) 138, arXiv:0707.2553 [hep-ph].
38. A. Denner, S. Dittmaier, T. Kasprzik and A. Muck, JHEP **0908** (2009) 075, arXiv:0906.1656 [hep-ph].
39. L. J. Dixon, Z. Kunszt and A. Signer, Nucl. Phys. B **531** (1998) 3 [hep-ph/9803250].
40. D. De Florian and A. Signer, Eur. Phys. J. C **16** (2000) 105, hep-ph/0002138.
41. J. M. Campbell, R. K. Ellis and C. Williams, JHEP **1107** (2011) 018, arXiv:1105.0020 [hep-ph].
42. W. B. Kilgore and C. Sturm, Phys. Rev. D **85** (2012) 033005, arXiv:1107.4798 [hep-ph].
43. A. D. Martin, R. G. Roberts, W. J. Stirling and R. S. Thorne, Eur. Phys. J. C **39** (2005) 155, hep-ph/0411040.
44. C. Buttar, J. D’Hondt, M. Kramer, G. Salam, M. Wobisch, N.E. Adam, V. Adler, A. Arbuzov *et al.*, “Standard Model Handles and Candles Working Group: Tools and Jets Summary Report”, arXiv:0803.0678 [hep-ph].
45. C. M. Carloni Calame, G. Montagna, O. Nicrosini and M. Treccani, JHEP **0505** (2005) 019 [hep-ph/0502218].
46. T. Sjostrand, S. Mrenna and P. Z. Skands, JHEP **0605** (2006) 026, hep-ph/0603175.

47. U. Baur, Phys. Rev. D **75** (2007) 013005, hep-ph/0611241.
48. G. Bell, J. H. Kuhn and J. Rittinger, Eur. Phys. J. C **70** (2010) 659, arXiv:1004.4117 [hep-ph].
49. G. Aad *et al.* [ATLAS Collaboration], Phys. Lett. B **705** (2011) 415, arXiv:1107.2381 [hep-ex].
50. S. Chatrchyan *et al.* [CMS Collaboration], Phys. Rev. D **85** (2012) 032002, arXiv:1110.4973 [hep-ex].
51. T. Sjostrand, S. Mrenna and P. Z. Skands, Comput. Phys. Commun. **178** (2008) 852, arXiv:0710.3820 [hep-ph].
52. A. D. Martin, W. J. Stirling, R. S. Thorne and G. Watt, Eur. Phys. J. C **63** (2009) 189, arXiv:0901.0002 [hep-ph].
53. A. B. Arbuzov and R. R. Sadykov, J. Exp. Theor. Phys. **106** (2008) 488, arXiv:0707.0423 [hep-ph].
54. S. Brensing, S. Dittmaier, M. Kramer, 1 and A. Muck, Phys. Rev. D **77** (2008) 073006, arXiv:0710.3309 [hep-ph].